http://dx.doi.org/10.5012/bkcs.2014.35.7.1999

Hydrothermal Synthesis of Indium Tin Oxide Nanoparticles without Chlorine Contamination

Hai Wen Wang, Guo Dong Xu, Jian Rong Zhang,† and Xin Yin*

Department of Chemistry, East China University of Science and Technology, Shanghai 200237, China
**E-mail: yoshikiyin@ecust.edu.cn*
†Ningbo Jinxin Advanced Materials Ltd, Zhejiang 315303, China
Received December 27, 2013, Accepted March 10, 2014

Indium tin oxide ($In_2Sn_{1-x}O_{5-y}$) nanoparticles were synthesized by hydrothermal method from stable indium tin acetylacetone complexes and postannealing at 600 ºC. The absence of chlorine ions shortened the synthesis process, decreased the particle agglomeration and improved the particle purity. The introduced complexing ligand acetylacetone decreased the obtained nanoparticle size. The improved powder properties accelerated the sintering of the $In_2Sn_{1-x}O_{5-y}$ nanoparticles and reached a relative density of 96.4% when pressureless sintered at 1400 ºC.

Key Words : Indium tin oxide, Synthesis, Nanoparticle, Sintering

Introduction

Indium tin oxide (ITO) is the most widely used transparent conductive oxide (TCO) owing to its combination of high conductivity and high optical transparency in the visible region. Most of the transparent electrodes (*e.g.* in display, OLEDs, and solar cells) are made of ITO films. ITO also reflects infrared radiation and can be used as heat mirrors to reduce energy consumption.[1-5] Almost all the ITO materials are applied in the form of films and only a small amount is used in the form of particles added in the polymer to increase electrical conductivity.[6] Among the various techniques to deposit ITO films, chemical vapor deposition, vacuum evaporation, spray pyrolysis, and the newly developed printing methods, magnetron sputtering is the most preferred because it is advantageous in controllability of deposition conditions and adaptability to large area.[1,2] Large area deposition of ITO films has been the trend from the view of market demand and cost. It is well known that the sputtering efficiency and the properties of the ITO films are strongly dependent on the characteristics of the ITO target and the most important parameter is the target density.[1,3,4,5,7] Study for higher ITO target density, more microstructural homogenesity and lower fabrication cost has been devoted too much works. Obtaining monodispersed indium tin oxide particles with high sinterability and high purity is of the first importance for the ITO materials.

Coprecipitation is a simple and economic method to obtain ITO nanoparticles and almost all the ITO powders appeared in the market are produced by this method.[8,9] But coprecipitation method has several drawbacks. The chemical homogenesity is difficult to control and the indium tin hydroxide precursors require calcination to be transformed to oxide which leads to agglomerates. Previous study showed that the resistivity of SnO_2 phase is several orders of magnitude higher than that of ITO matrix. So, a less homogeneous ITO target results in nodule formation and in turn decreases the target utility and film deposition efficiency.[3] The state of powder aggregation strongly affects the sintering behavior. The increase of aggregate content decreases the green density, increases the sintering temperatures and decreases the microstructural homogeneity.[10] In order to decrease the particle aggregation, emulsion techniques were developed to synthesize the ITO nanoparticles.[11,12] Buhler *et al*. obtained conductive ITO nanocrystals by microwave-assisted coprecipitation in ionic liquids (ILs).[2] But these methods need comparatively large amount of organic compounds which make the hydroxide washing step very tedious and increases the cost sharply. No suppliers acknowledge that their ITO powders are produced by emulsion methods. To overcome the drawbacks of coprecipitation, hydrothermal method is introduced to synthesize oxide powders and also applied to ITO particles. The main advantages of hydrothermal synthesis are homogeneous nucleation which leads to chemical homogeneity; avoidance of calcination step which decreases the degree of aggregation.[13] Yanagisawa *et al.* hydrothermally treated the indium tin hydroxides obtained by coprecipitation, followed by calcination at 500-1000 ºC and obtained $In_2Sn_{1-x}O_{5-y}$ nanoparticles. They pressurelessly sintered the powder compact at 1450 ºC and obtained a relative density of 93%, which is the highest value in the literature.[5,14,15] This result revealed that the hydrothermally obtained indium tin oxide powder showed high sinterability. In order to decrease the hydrothermal pressure, Xu *et al.* changed the mineralizer NH_3 to NaOH and obtained the indium tin oxide nanoparticles after heat-treated at 500 ºC.[16] But the introduced Na^+ ions bring several problems, the total impurities were over 100 ppm, a low limit value commercial ITO powder requested. The Na^+ impurity content was about 30 ppm and this would strongly deteriorate the ITO film conductivity when these powders were used to fabricate ITO sputtering target. Yanagisawa and Xu used indium tin hydroxides as the

hydrothermally starting materials and the hydroxides underwent dissolution-precipitation transformation during the hydrothermal process which needed a high temperature and a long period of time. For example, Yanagisawa *et al.* used a 300 °C[14,15] and Xu *et al.* decreased the hydrothermal temperature to 250 °C.[16] Fang *et al.* tried to synthesize ITO nanoparticles in sub- and supercritical water from the mixture solution of $SnCl_4$ and $InCl_3$.[17] They only obtained a mixture of SnO_2 and In_2O_3 nanoparticles, which may be ascribed to the strong acidic synthesis condition. The ITO powders produced by the traditional wet chemical methods usually need an additional reducing treatment to increase the particle conductivity. Choi *et al.* changed the hydrothermal solvent water to ethylene glycol (solvothermal) and obtained bluish conductive cubic ITO nanopowders, directly.[13] Indium nitrate or chloride and tin chlorides are commonly used as the starting materials because they are inexpensive and easy to control the synthesis parameters. But the chlorine ions are very difficult to be rinsed from the colloidal precipitates even after ten times of washing and such a procedure is very inefficient. It is well known that the presence of the chlorine ions in the oxide powders forms hard agglomeration between nanoparticles, hinders powder densification and decreases the particle purity. Kim *et al.*[8] found that the introduced chlorine ions changed the morphology of the obtained ITO nanoparticles from spherical to needle-like, which is disadvantageous for ITO densification. The presence of high concentrated chlorine ions in the autoclave is very corrosive under the high temperature and high water pressure working condition. Indium and tin alkoxides are good choice to avoid the contamination of chlorine ions, but they are very expensive, water-sensitive and hard to control the synthesis process.[18]

In the present study, we synthesized indium tin oxide nanoparticles by a novel hydrothermal method. We firstly synthesized stable indium tin complexing solution without introducing chlorine ions. Then hydrothermally treated the solution at 200 °C for 10 h. The obtained particles were calcined at 600 °C and the yellowish indium tin oxide nanopowders were produced. We sintered the powder in air and reached a relative density of 96.4% at 1400 °C.

Experimental

The indium tin oxide nanoparticles were synthesized by a novel hydrothermal method. Metal indium (5 N purity) was dissolved in concentrated HNO_3. Metal tin (5 N purity) was dissolved in 8 $molL^{-1}$ HNO_3 in ice water bath and then mixed these two solutions. Calculated amount of acetylacetone (acac) (molar ratio of acac/([In] + [Sn]) was set at 2:1) was added to the above solution. Aqueous ammonia (25 wt %) was added dropwise into the solution to adjust pH to ~7. Then this solution was transferred into a sealed stainless Telfon-lined autoclave with a capacity of 100 mL and maintained at 200 °C for 10 h. After air-cooled to room temperature, the derived black product was washed with distilled water and absolute alcohol, repeatedly. The yellowish indium tin oxide nanoparticles were obtained after heat-treated in muffle furnace at 600 °C for 3 h.

The indium tin oxide nanopowders (SnO_2 content was 10 wt %) were formed into pellets of 10 mm in diameter and 1.5 mm thick by uniaxial pressing, followed by cold isostatic pressing (CIP) at a pressure of 200 MPa. Then the compacts were sintered at different temperatures for 5 h in air at a constant heating rate of 5 °C/min and obtained green to black ITO ceramics.

The phase structure of the indium tin oxide nanoparticles and sintered ceramics were characterized by powder X-ray diffraction (XRD, D/max 2550 V, Rigaku, Tokyo, Japan) (Cu Kα, λ = 1.5418 Å). Weight variation upon thermal treatment of the hydrothermally obtained particles was characterized by simultaneous thermogravimetry and differential scanning calorimetry (TG-DSC, Netasch STA 449 analyser, Germany). The specific surface area (A) of the indium tin oxide particles were measured by multipoint Brunauer, Emmett and Teller adsorption. (BET, Micrometritics ASAP 2010, London, British) The morphology of the indium tin oxide nanoparticles was examined by transmission electron microscopy (TEM, JEOL-2100F, Tokyo, Japan). The microstructures of the polished and thermally etched ITO ceramics were observed by scanning electron microscope (SEM, JSM 6700F, Tokyo, Japan). The density of the ITO ceramics was determined using Archimedes' method in water.

Results and Discussion

Figure 1 presents the typical TG-DSC curves of the hydrothermally obtained powders (molar ratio of Sn/In at 9 atomic%). The first weight loss of 6.5% (from room temperature to 130 °C) with an endothermic feature is attributed to the evaporation of the adsorbed water and residual EtOH. The second weight loss of 23% (*ca.* 400 °C) with a heavy exothermal feature at 340 °C originates from the oxidation of the residual carbon (the black appearance of the hydrothermally obtained particles revealed that acac was decomposed under the hydrothermal condition). Above 400

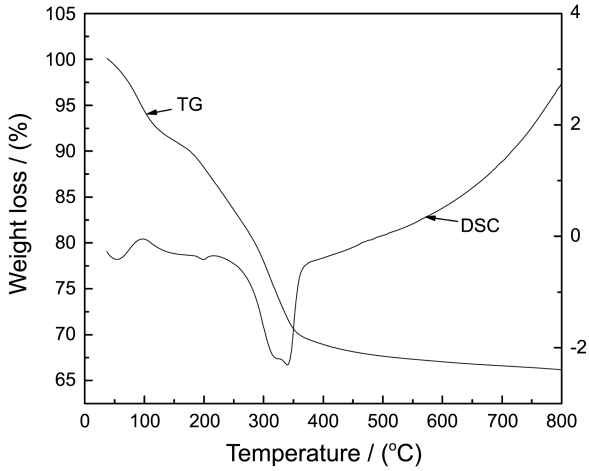

Figure 1. TG-DSC curves of the hydrothermally obtained powders.

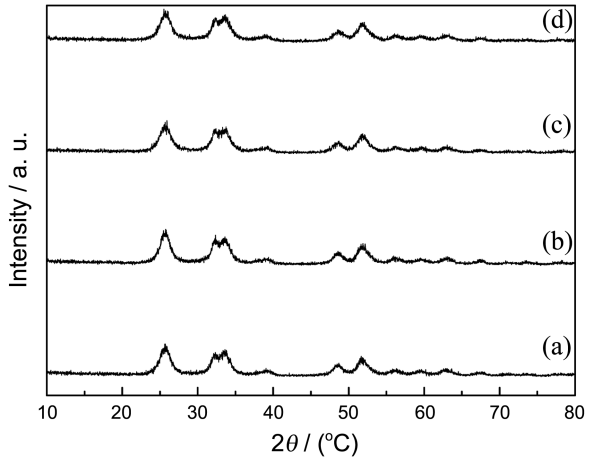

Figure 2. XRD patterns of the hydrothermally obtained InOOH nanoparticles with different tin/indium molar ratios (a) 3 atomic%; (b) 6 atomic%; (c) 9 atomic%; (d) 12 atomic%.

°C, the weight remains constant and has no endo- or exothermal character, these results reveal that the particles transformed into stable phase before 400 °C.

Figure 2 shows XRD patterns of the hydrothermally synthesized particles with different tin doping content. All peak positions correspond well with the reflections of orthorhombic InOOH (JCPDF 17-0549). This result agrees with the particles obtained by the hydrothermal method from the indium tin hydroxide precursors but we decreased the hydrothermal temperature from 250 °C or 240 °C to 200 °C.[5,15,16] In our experiment, the free indium and tin ions are released from the stable complexing ions steadily under the hydrothermal conditions and then nucleated and grew into the InOOH particles. In the hydroxide precipitates hydrothermal process, the hydroxides $In(OH)_3$ and $Sn(OH)_4$ underwent a dissolution-precipitation process and transformed to InOOH phase. This comparison revealed that hydrothermal treatment is essential for the partly dehydrated InOOH formation. Kim *et al.*[19] found that precipitated $In(NO_3)_3$ and $SnCl_4$ at a temperature of 5 °C also obtained the InOOH phase, which revealed that a relatively low temperature accelerated the $In(OH)_3$ dehydration. The XRD peak position shifted steadily toward lower angle side with the increase of tin doping level, indicating an increase in the lattice parameter. We failed to calculate the lattice parameters by least-squares refinement because of the relatively low particle crystallinity. The particle crystallinity decreased with the increase of tin content, in agreement with what Yanagisawa *et al.*[14] observed. The average crystallite size calculated by the Scherrer equation based on the width of the (100) reflection plane shows that the crystallte size is about 6.3 nm for the 3 atomic% doping level and decreases to 4.5 nm when doping content was 12 atomic%.

Figure 3 is the TEM images of the 3 atomic% and 12 atomic% tin doped InOOH nanoparticles. The particle size ranges from 5 to 9 nm for the 3 atomic% doped sample and decreases to 3 to 6 nm for the 12 atomic% InOOH particles. The particles are weakly connected with one another

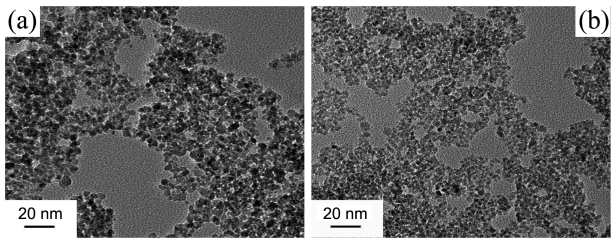

Figure 3. TEM photographs of the hydrothermally obtained InOOH nanoparticles with tin/indium molar ratios at (a) 3 atomic%; (b) 9 atomic%.

ascribed to the high surface energy of the nanoparticles and the adhesive decomposed acac residuals. Yanagisawa *et al.* obtained the InOOH particles in the size of 15 nm with heavy degree of agglomeration. Yin *et al.*[20] suggested that in the hydrothermal process, the complex ions coordinated to the metal ions, making the nucleation completed at the early stage of the hydrothermal process and inhibiting the crystal growth.

The hydrothermally obtained tin doped InOOH nanoparticles were calcinated at 600 °C to be transformed to indium tin oxide particles. Figure 4 shows XRD patterns of the particles. The InOOH phase has been dehydrated completely to the substitutional vacancy type interstitial solid solution of $In_2Sn_{1-x}O_{5-y}$, Agreed with what the previously obtained.[5,14,15] The crystallite size calculated from the plane 2θ at 31° and the specific surface area of the particles with different tin content are presented in Figure 5. The crystallite size decreases from 17.1 nm gradually to 12.3 nm with the increase of tin content from 3 atomic% to 12 atomic%, while the specific area increases from 35.7 m^2g^{-1} to 56.9 m^2g^{-1}. TEM images provided in Figure 6 show that the 3 atomic% doped $In_2Sn_{1-x}O_{5-y}$ nanoparticles have a size of 15 to 23 nm and size of 10 to 17 nm for the 9 atomic% tin doped sample, growing 2 to 3 times larger than the just hydrothermally obtained InOOH particles. The particles are well-faceted and

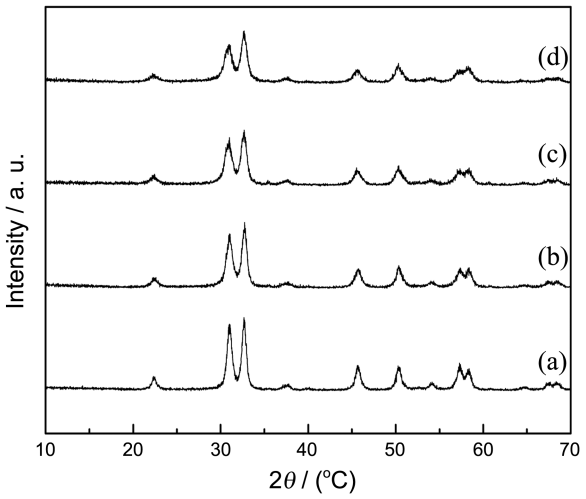

Figure 4. XRD patterns of the $In_2Sn_{1-x}O_{5-y}$ nanoparticles with different tin/indium molar ratios (a) 3 atomic%; (b) 6 atomic%; (c) 9 atomic%; (d) 12 atomic%.

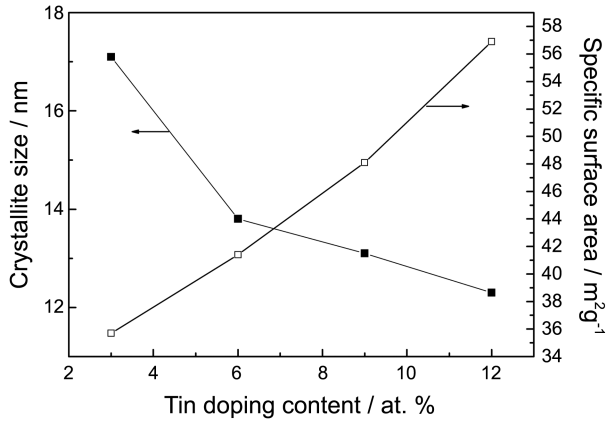

Figure 5. Crystallite size and specific surface area of the $In_2Sn_{1-x}O_{5-y}$ nanoparticles as a function of the tin doping content.

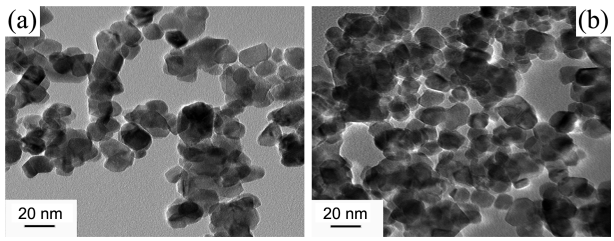

Figure 6. TEM photographs of the $In_2Sn_{1-x}O_{5-y}$ nanoparticles with tin/indium molar ratios at (a) 3 atomic%; (b) 9 atomic%.

show high degree of crystallinity and this is advantageous for particle sintering.

Figure 7 shows the relative density of the fabricated ITO ceramics at different sintering temperatures. A relative density of 77.8% is obtained at 1000 °C and this is the highest value for the ITO particles sintered at this temperature in the literature. Yanagisawa *et al.* sintered the $In_2Sn_{1-x}O_{5-y}$ particles with different tin content at 1250 °C and all the relative density values were below 60%.[14] Sawada *et al.* used ITO particles with size of 2.97 μm and no densification was observed when sintered up to 1500 °C.[21] This comparison

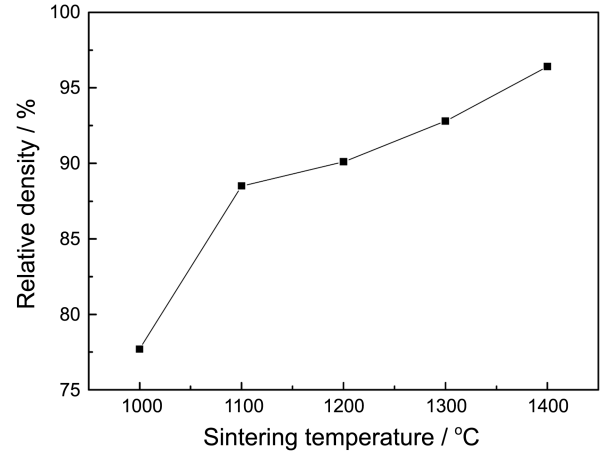

Figure 7. Relative density of the fabricated ITO ceramics as a function of sintering temperature.

indicates that our $In_2Sn_{1-x}O_{5-y}$ nanoparticles exhibit high sinteribility, which is ascribed to the small particle size, low degree of particle agglomeration and free from chlorine contamination. As is well known, the driving force for densification is lowering the surface free energy by the elimination of solid-vapor interface. The smaller the particle size is, the higher the surface free energy is, the easier of surface atom diffusion between neighbour particles. The densification rate, dρ/dt, is dependent on the grain size (d), as predicted by several well-known sintering models: dρ/dt $\propto$ (1/d)n, where the grain-size exponent n has a valve of 3 or 4, depending on the dominant diffusion path. A decrease in the grain size by a factor of 2 will increase the densification rate by approximately one order of magnitude.[22] So, the synthesis of nanoparticles is of first importance in fabrication ceramics having improved properties. But nanoparticles are not always beneficial for sintering, the agglomeration which is usually present in the nanoparticles due to the high particle surface free energy retards the compaction of the particles, decreases the sintering rates and leads to inhomogeneous microstructure in the ceramics.[23] Figure 8(a) is SEM photograph of the ITO pellet sintered at 1000 °C. The particles sintered by neck formation and the particle size grew to about 150 nm. XRD pattern of the pellet presented in Figure 9(a) reveals that during the sintering process the $In_2Sn_{1-x}O_{5-y}$ phase has transformed to cubic In_2O_3 phase. Very small amount of SnO_2 is also observed in the XRD pattern which indicates that the solubility of Sn in In_2O_3 is under 10 wt % at 1000 °C. Similar result has been detected by several reports.[8,24] Further raising the sintering temperature increases the relative density of the ITO ceramics gradually and the highest value 96.4% was reached when sintered at 1400 °C. Figure 8(b) shows that the ceramics has a dense surface with a few small pores. The grain size is about 5.9 m and is about forty times larger than the 1000 °C sintered pellet. The grain growth is much faster in the final stage of densification when the density is above 90% TD.

Figure 9 shows the XRD patterns of the sintered ITO ceramics. Cubic In_2O_3 phase is the major phase in all patterns which indicates that the high temperature sintering accelerates $In_2Sn_{1-x}O_{5-y}$ phase transforming to cubic In_2O_3 (JCPDF 44-1087). Small amount of SnO_2 (JCPDF 41-1445) is detected in the ITO ceramics sintered up to 1200 °C and is not observed in the 1300 °C, 1400 °C sintered pellets. This result reveals that the tin ions precipitate in the form of SnO_2 when its content is above the solubility in In_2O_3 (the SnO_2

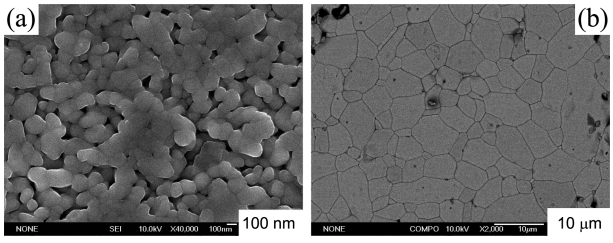

Figure 8. SEM micrographs of the ITO ceramics sintered at (a) 1000 °C and (b) 1400 °C.

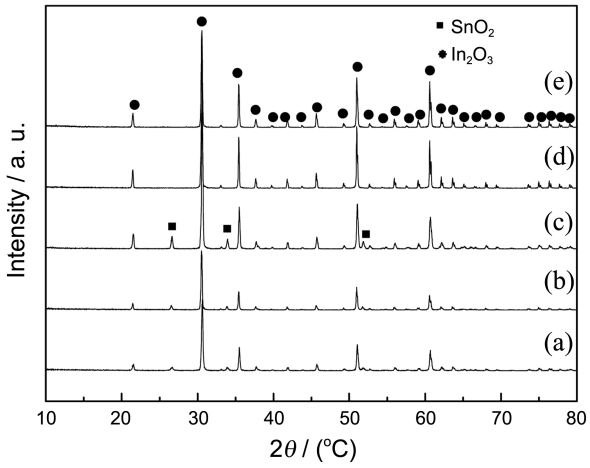

Figure 9. XRD patterns of the ITO ceramics (SnO_2 content is 10 wt %) sintered at different temperatures (a) 1000 °C; (b) 1100 °C; (c) 1200 °C; (d) 1300 °C; (e) 1400 °C.

content is 10 wt % in our sintered pellets). Previous studies indicated that SnO_2 showed a high evaporation rate for temperatures higher than 1200 °C due to the peritectic decomposition according to the reaction:[22]

$$SnO_2\ (s) \rightarrow SnO\ (g) + 1/2\ O_2\ (g) \quad (1)$$

So the disappearance of SnO_2 phase in the 1300 °C, 1400 °C sintered pellets may be ascribed to the evaporation of the precipitated SnO_2. The sublimation of SnO_2 in ITO is accelerated when temperature is above 1200? has also been observed directly by Palmer *et al.*[25] The XRD patterns also show the peak sharpening increases with the increase of sintering temperature which witnesses the growth of the ITO grains.

Conclusion

Indium tin oxide ($In_2Sn_{1-x}O_{5-y}$) nanoparticles with particle size of about 15 nm were successfully synthesized by hydrothermal and post heat treatment. We obtained the stable indium tin acetylacetone complexes to avoid the contamination of the chlorine ions without using metal alkoxides. The hydrothermal treatment of stable indium tin acetylacetone complexes free from chlorine ion contamination bring several good results: greatly shorten the particle washing steps, improve the powder purity, decrease the nanoparticle size, decrease the particle agglomeration and increase the particle sinterability.

Acknowledgments. The authors are grateful to financial support from National Natural Science Foundation of China (No. 50902049).

References

1. Utsumi, K.; Ligusa, H.; Tokumaru, R.; Song, P. K.; Shigesato, Y. *Thin Solid Films* **2003**, *445*, 229.
2. Buhler, G.; Tholmann, D.; Feldmann, C. *Adv. Mater.* **2007**, *19*, 2224.
3. Nakashima, K.; Kumahara, Y. *Vacuum* **2002**, *66*, 221.
4. Nadaud, N.; Nanot, M.; Boch, P. *J. Am. Ceram. Soc.* **1994**, *77*, 843.
5. Udawatte, C. P.; Yanagisawa, K. *J. Am. Ceram. Soc.* **2001**, *84*, 251.
6. Cho, Y. S.; Yi, G. R.; Hong, J. J.; Jang, S. H.; Yang, S. M. *Thin Solid Films* **2006**, *515*, 1864.
7. Omata, T.; Kita, M.; Okada, H.; Matsuo, S. O. Y.; Ono, N.; Ikawa, H. *Thin Solid Films* **2006**, *503*, 22.
8. Kim, S. M.; Seo, K. H.; Lee, J. H.; Kim, J. J.; Lee, H. Y.; Lee, J. S. *J. Euro. Ceram. Soc.* **2006**, *26*, 73.
9. Kim, B. C.; Lee, J. H.; Kim, J. J.; Lee, H. Y.; Lee, J. S. *Mater. Res. Bull.* **2005**, *40*, 395.
10. Barringer, E. A.; Bowen, H. K. *J. Am. Ceram. Soc.* **1982**, *65*, C199.
11. Kim, D. W.; Oh, S. G.; Lee, J. D. *Langmuir* **1999**, *15*, 1599.
12. Kim, D. W.; Oh, S. G.; Yi, S. C.; Bae, S. Y.; Moon, S. K. *Chem. Mater.* **2000**, *12*, 996.
13. Lee, J. S.; Choi, S. C. *J. Euro. Ceram. Soc.* **2005**, *25*, 3307.
14. Udawatte, C. P.; Yanagisawa, K. *J. Solid State Chem.* **2000**, *154*, 444.
15. Yanagisawa, K.; Udawatte, C. P. *J. Mater. Res.* **2000**, *15*, 1404.
16. Xu, H. R.; Zhu, G. S.; Zhou, H. Y.; Yu, A. B. *J. Am. Ceram. Soc.* **2005**, *88*, 986.
17. Fang, Z.; Assaaoudi, H.; Guthrie, R. I. L.; Kozinski, J. A. *J. Am. Ceram. Soc.* **2007**, *90*, 2367.
18. Toki, M.; Aizawa, M. *J. Sol-Gel Sci. Tech.* **1997**, *8*, 717.
19. Seo, K. H.; Lee, J. H.; Kim, J. J. *J. Am. Ceram. Soc.* **2006**, *89*, 3431.
20. Yin, H. B.; Wada, Y.; Kitamura, T.; Sumida, T.; Hasegawa, Y.; Yanagida, S. *J. Mater. Chem.* **2002**, *12*, 378.
21. Suzuki, M.; Muraoka, M.; Sawada, Y.; Matsushita, J. *Mater. Sci. Engin. B* **1998**, *54*, 46.
22. Leite, E. R.; Cerri, J. A.; Longo, E.; Varela, J. A.; Paskocima, C. A. *J. Euro. Ceram. Soc.* **2001**, *21*, 669.
23. Dynys, F. W.; Halloran, J. W. *J. Am. Ceram. Soc.* **1984**, *67*, 596.
24. Gonzalez, G. B. *Ph.D thesis*, Northwest University, USA, 2003.
25. Palmer, G. B.; Poeppelmeir, K. R.; Mason, T. O. *Chem. Mater.* **1997**, *9*, 3121.